TURBOFAN BROADBAND NOISE PREDICTIONS BASED ON A ZDES CALCULATION OF A FAN-OGV STAGE

Cyril Polacsek, Majd Daroukh, Benjamin François, Raphael Barrier

TURBOFAN BROADBAND NOISE PREDICTIONS BASED ON A ZDES CALCULATION OF A FAN-OGV STAGE

Cyril Polacsek[1] Majd Daroukh[1] Benjamin François[2] Raphael Barrier[2]
[1] ONERA, The French Aerospace Lab, Numerical Aeroacoustic Team, 92320 Châtillon, France
[2] ONERA, The French Aerospace Lab, CFD Turbomachinery Team, 92190 Meudon, France
Cyril.Polacsek@onera.fr

ABSTRACT

This paper presents undergoing acoustic analyses of an hybrid RANS/LES calculation performed at ONERA in the framework of an European project TurboNoiseBB. The numerical approach proposed here relies on a Zonal Detached Eddy Simulation strategy that is applied to a fan module equipped with 20 rotor blades and 44 outlet guide vanes and tested in AneCom facility (Wildau, Germany). The ZDES method with detailed numerical set-up and aerodynamic flow features are discussed in a companion paper and the present one mainly focuses on acoustic analyses. Post-processed data are used to feed acoustic codes based on Amiet theory and Ffowcs-Williams and Hawkings analogy for which required inputs to assess rotor-stator interaction noise are the turbulence wake information and the unsteady pressure over the vane wall, respectively. The turbulent wake characteristics in terms of energy and spectral content are compared to hot-wire measurements. In particular radial profiles of turbulent velocity components and power spectrum density at selected duct height positions are analyzed, as well as integral and spanwise correlation length scales. Hence, sound power spectra in the bypass predicted by both acoustic codes are presented and compared to the experiment.

1. INTRODUCTION

Turbofan broadband noise is nowadays a major topic of concern for aircraft engine manufacturers as its prediction and reduction are both challenging tasks. In the fan module, the main contribution of the broadband noise (BBN) more particularly at approach operation point, is the interaction of the turbulent structures generated in the fan wakes with the outlet guide vanes (OGV). The present work is done in the framework of TurboNoiseBB project and is devoted to the BBN prediction of rotor-stator interaction (RSI) mechanism, based on an hybrid RANS/LES calculation applied to the ACAT1 turbofan model at approach conditions [1]. The ACAT1 fan is equipped with 20 blades and 44 vanes and has been tested in AneCom facility (Fig. 1) [2]. A dedicated instrumentation including hot-wire probes and in-duct/outside microphone antenna has provided data set that are used here for main aerodynamic and acoustic validations.

The CFD relies on a ZDES (Zonal Detached Eddy Simulation) that is detailed in a companion paper [1], describing the numerical set-up and first aerodynamic results, while the present one focuses on turbulent wake analyzes and first acoustic predictions. The turbulent fan wakes need to be simulated either by a RANS calculation able to estimate its main averaged characteristics i.e., turbulent kinetic energy and integral length scale, either by a turbulence scale resolved approach to get the statistical and spectral quantities i.e., RMS velocities, power spectral density (PSD), and correlation length scales. The choice of the approach is a trade-off between physical accuracy and numerical cost. The more challenging aspect concerns the assessment of turbulent wall pressure over the vane surface. Although the vane response can be modeled by means of analytical models based on Amiet theory (requiring important simplifications of the turbulent flow and the geometry), the strategy adopted here aims to directly capture both the turbulent wakes and the turbulent sources at vane walls. Because of the high Reynolds number involved (around one million), turbulence-scale-resolved simulations of a fan stage require an important computational effort. For this reason, such BBN simulations remain scarce in the literature. The LBM approach has been successfully applied on the NASA Source Diagnostic Test (SDT) case with quite impressive results [3]. For most current Navier-Stokes solvers, the use of a wall law (practically adopted in the LBM too) enables the reduction of the numerical effort, as done in wall-modeled LES (WMLES). WMLES technique has been recently performed in [4] on the NASA SDT case. An alternative way is to resort to hybrid RANS/LES approaches in which the whole boundary layer is solved with a RANS modeling. Hence, their numerical cost is much less dependent on the Reynolds number. The use of ZDES technique remains quite new for such applications. This approach has already been used by Bonneau *et al.* [5] for the prediction of turbofan broadband noise where only one fan blade was simulated. The present work is an extension of Ref. [5] by accounting for the OGV in the computational domain.

ZDES post-processed fields (turbulent wakes and turbulent pressure wall) are inputted in acoustic codes, briefly described in the paper, and respectively based on Amiet theory and Ffowcs-Williams and Hawkings (FWH) analogy. The present acoustic predictions are restricted to power spectrum densities (PSD) of sound power (PWL spectra) in the bypass duct, that are compared to RANS-based solutions also presented and discussed in a collaborative paper [6], and to experiment.

The paper is structured as follows:

- Section 2 briefly presents the CFD set-up with basic aerodynamics and data extraction for acoustics;
- Section 3 is devoted to advanced turbulent wake analyses, by showing iso-contour maps and radial profile comparisons, looking to cyclo-stationnary and turbulent contributions, and addressing the spectral content of the turbulent velocity fields (PSD and correlation length scales);
- Section 4 then gives a brief overview of the ONERA acoustic codes and their chaining to the ZDES, and first BBN predictions based on Amiet theory and FWH analogy are presented and compared to experiment;

Finally, work status and some conclusions are suggested.

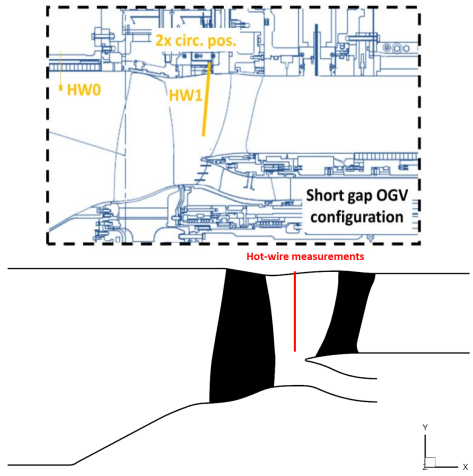

Figure 1. Meridional view of the fan module in AneCom rig (top) and CFD domain with hot-wire probes at HW1 position (bottom).

2. ZDES METHODOLOGY OVERVIEW AND DATA EXTRACTION FOR ACOUSTICS

2.1 CFD set-up

The configuration is studied at rig-scale (the outer radius of the fan is 0.42 m). The Inlet Guide Vanes (IGV) are not accounted for in the simulation because their contribution to the RSI noise is negligible compared to the fan-OGV contribution (the bypass ratio is around six). The configuration is studied at approach conditions (50% Nn, namely 3828.4 *rpm*) for which the RSI noise is dominant. The ZDES method developed by Deck [7] and implemented in *elsA* ONERA code [8] is used here. The DES mode 2 based on Spalart turbulence model adopted here is described in [1,8]. The convective flux discretization is treated with the AUSM (Advection Upstream Splitting Method) scheme with a third order limiter. The implicit time scheme is ruled by a second order scheme based on a Newton algorithm. Details about numerical parameters are given in Ref. [1].

An illustration of the RANS/DES zones on single channel computational domain is shown in Fig. 2, top. The actual number of blades/vanes (20/44) is unfavorable to reduce the computational domain to a few inter-blade channels. For unsteady RANS simulations, classical phase-lagged boundary conditions allow the reduction of the domain to a single blade channel. Because they are based on the usual Fourier decomposition, they are unadapted for the convection of broadband structures. Consequently, a more favorable option is to change the vane number of the OGV to get a suitable divisor and to permit the use of periodic boundary conditions instead. Even if the periodicity is still questionable for the turbulence structures between adjacent channels, the spectral content and the cascade effects (with respect to the turbulent sources) are believed to be conserved through these boundary conditions. This strategy has already been used by several authors [4]. For the present application, the number of vanes is thus reduced from 44 to 40. In order to keep the same flow pattern, the solidity is kept constant meaning that the chord is increased by 10%, the leading edge position being unchanged. This allows for the reduction of the computational domain to one fan channel and two OGV channels, with a negligible aerodynamic impact [1]. A sliding mesh treatment is performed at the interface between the rotating fan and the fixed OGV domains.

Concerning the mesh, it is structured and multi-blocks. Two sets of criteria were used to build the present grids. The first relies on internal best practices concerning the use of the DES mode 2. The cell size must verify Δx^+, Δy^+, $\Delta z^+ < 200$ in the free shear flow areas and first wall mesh size verifies $\Delta y^+ \leq 1$. The second criterion relies on the hydrodynamic wave length. A criterion of 20 points per wavelength leads to a mesh spacing requirement of 0.25 mm at 20 kHz, giving rise to a mesh of 3 billions cells. Practically, the selected cell size was 0.5 mm, ensuring a sampling of 20 points at 10 kHz and a total cell number restricted to 380 millions. A sectional view of ZDES mesh at mid-height (with duplicated blade channel) is shown in Fig. 2, bottom The complete grid (not shown) is extended 4 blade chords upstream and 3 vane chords downstream and is rapidly stretched in both directions (only visible upstream here) so that the last cell size reaches 3 cm and 2 cm respectively. Note that this stretching technique, aiming to increase the numerical dissipation, is currently used at ONERA for turbomachinery aeroacoustic applications in order to palliate the ineffective 1D characteristics-based non-reflecting boundary condition mostly implemented in CFD solvers (as in *elsA*) when using implicit schemes.

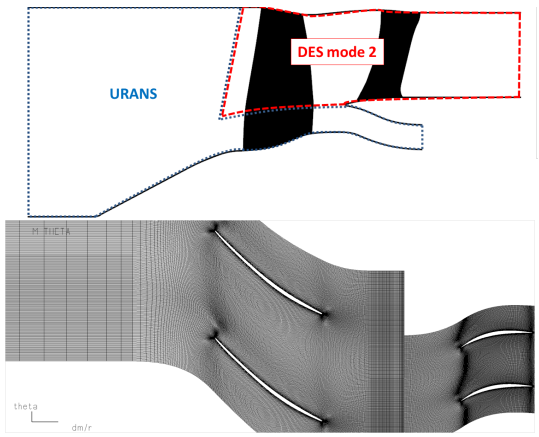

Figure 2. URANS and DES zones (top) and blade-to-blade section mesh with 1 over 2 pts. shown (bottom).

2.2 Basic flow visualizations and aerodynamic performances

Figure 3 (top), presents a visualization of the instantaneous flow field around the fan blade: surfaces of iso-values of the Q-criterion colored by the axial momentum are displayed. It highlights the zonal solving (RANS flow in the primary region). Because the flow separates at the leading edge of the fan for this operating point, turbulent structures are generated from there and are convected downstream. The high grid density enables to capture small turbulent structures. A visualization of vorticity magnitude fields on an iso-radius surface and on a transverse slice upstream the OGV are shown in Fig. 3 (bottom), left and right, respectively. The thick black lines (left) depicts the areas in which the shielding function f_d [1] equals 0.95, thus defining the border between the RANS solving (in the boundary layer) and the LES solving (in the free shear flow areas). For both fan and OGV blades, the RANS solving is found able to encompass the whole boundary layer, and the turbulent wakes seem to convect correctly through the periodic boundaries up to the OGV domain.

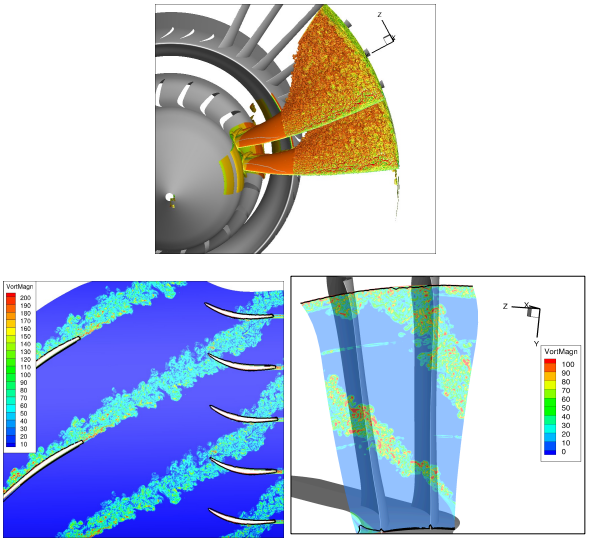

Figure 3. Iso-value surfaces of the Q-criterion around the fan blades (top) and of vorticity magnitude fields on an iso-radius slice (bottom, left) and on a transverse slice upstream the OGV (bottom, right).

The aerodynamic performances are quite well retrieved by the simulation as shown in Table 1. Small discrepancies on the secondary mass flow rate are due to the difficulty to monitor it with the DES solving. More details about convergence and basic aerodynamic analysis can be found in Ref. [1].

	Measurements	ZDES
Primary massflow [kg/s]	6.41	6.44
Secondary massflow [kg/s]	48.76	49.26
Secondary pressure ratio	1.108	1.106

Table 1. Comparison of aerodynamic performances.

2.3 Data extraction for acoustics

The first objective of these advanced simulations is to accurately capture the flow unsteadiness and the main turbulent contents involved in the RSI mechanism. In order to check the flow properties issued from the ZDES by comparison with available HW measurements and to provide the required inputs to the acoustic post-processing, data extractions over selected surfaces have been performed during the simulation [1]. The main analyses are realised at HW1 plane (Fig. 1), located at axial position X = -2.685 m. The most useful extracted quantity here is the 3-component velocity field. Same data have been extracted along a curved plane closely aligned (5 mm upstream) to the OGV leading edge to feed the Amiet-based tool (in-house code *TinA*) as discussed in Sections 3 and 4. Skin surfaces over the blade/vane walls provide the required inputs (unsteady wall pressure) to the FWH-based solver (in-house code *FanNoise*). Additional extractions along slices upstream the rotor and downstream the stator will be used for future complementary analyses (not discussed here). All the data are extracted at a sampling frequency of 100 kHz, namely one time step over 30, and a maximum duration time of 2.8 revolutions (56 fan blade passages), allowing to perform PSD analyses averaged over 12 blocks with a frequency resolution equal to 273 Hz (without overlapping). Unfortunately, the simulation could not be performed on a longer duration time (as initially planned) for robustness reasons. Indeed, as discussed in Section 4, ZDES iterations had to be stopped at 2.8 revs. because of numerical instabilities generated at some radial stations of the sliding grid interface, revealed by the horizontal streaks visible in Fig. 3 (right), that could pollute the unsteady solution.

3. TURBULENT WAKE ANALYZES

3.1 Cyclo-stationnary fields

First flow analyses are devoted to cyclo-stationnary fields in terms of 2D contour maps (slices) at HW1 plane. Present results are focused on mean velocity and RMS turbulent velocity fields. Only one blade passage is solved in the ZDES (as the turbulent flow is assumed to be actually periodic from blade-to-blade), corresponding to a 2-vanes sector with the modified 40-vanes OGV adopted in the numerical set-up. 360° maps are simply obtained by duplicating the 1-blade-channel numerical solution over the 20 blades (Fig. 4, left), whereas the phase-locked HW measurements assess full 360° maps (Fig. 4, right) that can reveal significant blade-to-blade deviations (due to imperfect test conditions). Comparisons of phase-locked contour maps averaged and duplicated over 3-blade channels (Fig. 5) show a quite good agreement between ZDES and experiment for axial component (same trend is found for tangential and radial components).

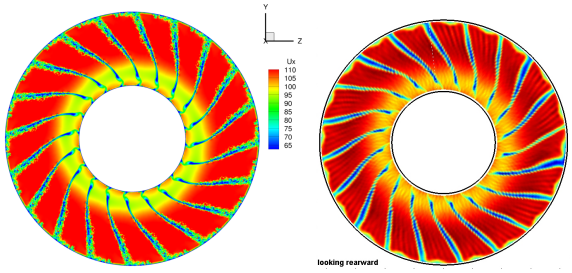

Figure 4. 360° maps of axial velocity: instantaneous ZDES solution (left) and phase-locked HW measurements (right).

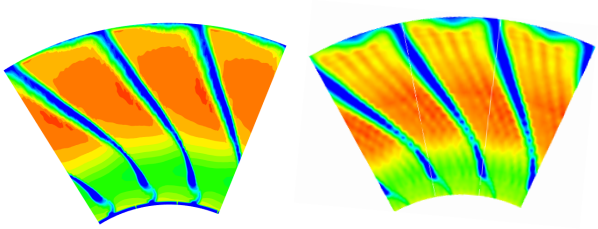

Figure 5. Phase-locked iso-contour maps of axial velocity issued from ZDES (left) and averaged experiment (right) duplicated over 3-blade channels.

Similar analyses on turbulent velocity fields are shown in Fig. 6, highlighting blade-to-blade level deviations in the measurements (Fig. 6, top) probably due to non-identical blades (slight geometry defects) or non-perfectly axisymmetric turbulent inflow conditions. Results for other components (only discussed in section 3.2 for sake of conciseness) display almost the same patterns with close levels than those observed on axial component, which tends to confirm that isotropic assumption currently adopted (in the sense of energy) is roughly valid. However, the numerical predicted levels are found to be above the experiment arguing for an over-estimation of the turbulent wake intensity by the ZDES. In fact, this level offset was recently attributed to the limited bandwidth of available HW probes (cut-off frequency around 7-8 kHz) giving rise to an under-prediction of RMS values of about 1.5 factor. This point is more discussed in Sections 3.2 and 3.3.

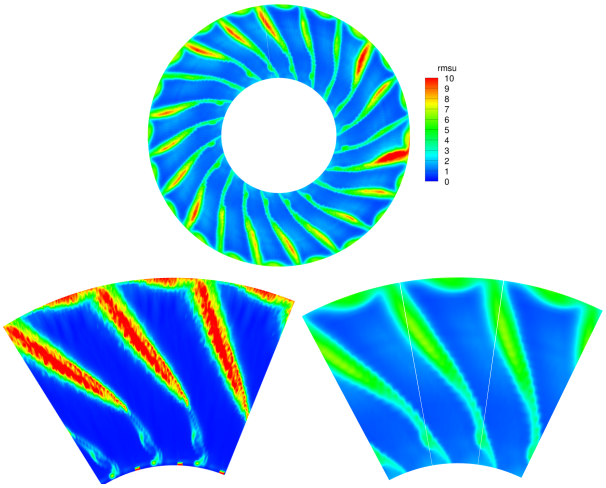

Figure 6. Comparison of RMS turbulent velocity fields (axial component): Phase-locked iso-contour maps issued from ZDES (left) and from 360° (top) and averaged (right) experiment.

3.2 Averaged radial profiles

Previous phase-locked results are circumferentially averaged to assess radial profiles. ZDES vs. experiment comparisons of mean velocity profiles are presented in Fig. 7, showing a very good agreement for axial and tangential components (same result for radial velocity). Similar analyses are proposed in Fig. 8 for RMS turbulent velocities by overplotting the experimental profiles obtained when applying the 1.5 factor correction (estimated from Parseval identity and integration of velocity PSD up to 8.5 kHz, as discussed in Section 3.3). A satisfactory matching is observed when adopting this correction, more particularly on the tangential component (Fig. 8, right).

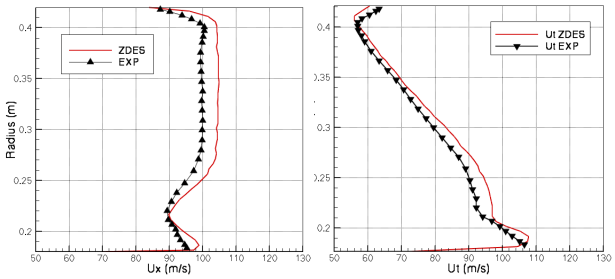

Figure 7. ZDES vs. experiment mean velocity profiles for axial (left) and tangential (right) components.

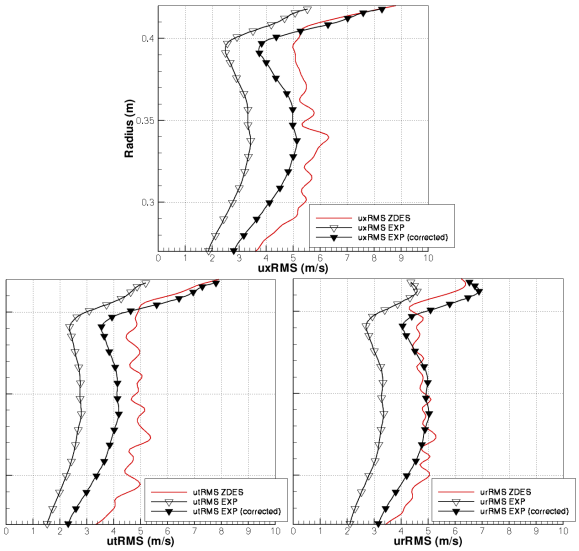

Figure 8. ZDES vs. raw and corrected experiment of RMS turbulent velocity profiles: axial (top), radial (bottom, left) and tangential (bottom, right) components.

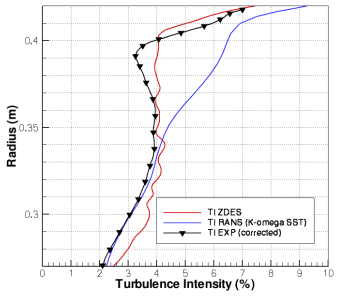

Figure 9. Comparison of turbulence intensity profiles assessed by ZDES, RANS and corrected experiment.

Turbulence intensity (TI) profiles provided by ZDES are compared to the so-corrected measurements in Fig. 9, in which a RANS-based solution (using k-ω Menter SST model) is also plotted. It is clearly observed that the ZDES-based solution better fits the experimental profile in the upper part of the vein up to the tip.

3.3 Velocity spectra and correlation length scales

Next results are devoted to PSD and correlation length scale analyzes. PSD are obtained using at least 10 averages with or without Welch method (50% overlapping) ensuring a frequency spacing of 273 Hz with the available signal duration. Comparisons to experiment at mid-height are proposed in Fig. 10, for axial (Fig. 10, left) and tangential (Fig. 10, right) turbulent velocity components (and using a Log axis scale limited to 20 kHz). Information about signal processing performed by DLR in AneCom tests can be found in [2]. One should note that tonal contribution (BPF harmonics) is included in the present measurement data set, whereas the cyclo-stationnary part was removed in the numerical solution. Theoretical PSD based on von-Karman (VK) spectrum model, with TI and turbulence length scale (TLS) values issued from RANS calculations (and adjusted to better fit the experiment), are addressed too. The ZDES spectrum is found to be in a good agreement with the experiment with respect to the maximum level "plateau", particularly for the tangential component, and is displaying a level attenuation slope not far from the VK one. However, although the ZDES slope is weaker, the experiment reveals a strong and questionable level attenuation slope beyond 7-8 kHz (see black dashed line), getting far away from expected VK -5/3 power law.

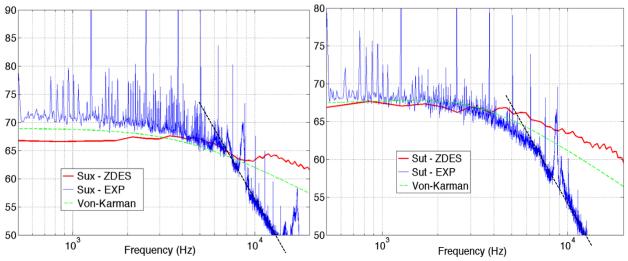

Figure 10. PSD (dB/Hz) of turbulent velocity (50% H) issued from ZDES, compared to VK and experimental spectra: axial (left) and tangential (right) components.

This unphysical attenuation was recently attributed to an inappropriate cut-off frequency of hot wire probes (enlarged diameter justified by mechanical constraints and probe damages during AneCom tests). Consequently, RMS turbulence levels issued from the measurements are underpredicted by a factor that can be roughly set equal to 1.5 (estimated from theoretical -5/3 power law). The PSD shape issued from ZDES is a bit more flat compared to the theoretical VK slope achieved here by setting a TLS value around 5 mm. This discrepancy is more pronounced in the tip region, tending to show that the ZDES provides lower TLS values (closer to 2 mm) than the one issued from a VK spectrum adjusted to fit the measurements (up to the cut-off frequency) and more in the range of 5-6 mm. This trend seems to be confirmed by the correlation scale analyzes, for which an assessment of TLS issued from ZDES can be estimated using zero time-shift cross-correlation function (applied to the streamwise velocity component) and Taylor's assumption. The radial profile of this length scale at HW1 position is plotted in Fig. 11 and compared to those issued from RANS (k-ω Menter SST) solution and deduced from current formula following Pope [9] and Jaron [10] and detailed in Ref. [6]. It can be observed that RANS-based TLS are increasing in the upper part of the duct and only decreasing near the casing wall, whereas ZDES solution predicts a significant decrease of TLS beyond r = 0.31 m up to the tip. This inverse trend is not easy to explain and more investigations should be done.

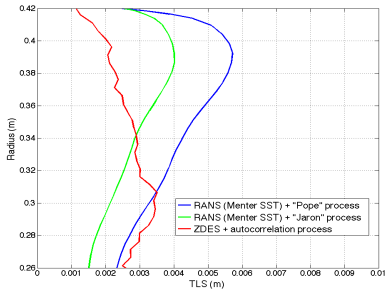

Figure 11. TLS profile obtained from ZDES (in red) and compared to RANS-based solutions.

As discussed in Section 4, a quite important quantity related to the turbulent wake trimming the RSI noise generation is the spanwise frequency-dependent correlation length scale (denoted ℓ_r here). It is obtained from the radial integration of the coherence function (root mean square), γ, applied to the upwash velocity component, u_n, as follows [11]:

$$\gamma(f,r_{12}) = \frac{\left|\left\langle u_n(f,r_1)u_n^*(f,r_2)\right\rangle\right|}{\left[S_{u_nu_n}(f,r_1)S_{u_nu_n}(f,r_2)\right]^{1/2}} ; \ell_r(f) = \int_0^\infty \gamma(f,r_{12})dr_{12} \quad (1)$$

The coherence function is practically assessed by extracting a radial line at constant angular station and by splitting the field into 10 radial strips. Spanwise correlation length scales are shown in Fig. 12, for 3 radial stations (20% H, 50% H and 90% H), and compared to the theoretical expression related to VK spectrum and using TLS profile based on Pope (see Fig. 11, left):

$$\ell_y(f) = \frac{8\Lambda}{3}\left(\frac{\Gamma(1/3)}{\Gamma(5/6)}\right)^2 \frac{(k_c/k_e)^2}{\left[3+8(k_c/k_e)^2\right]\sqrt{1+(k_c/k_e)^2}} \quad (2)$$

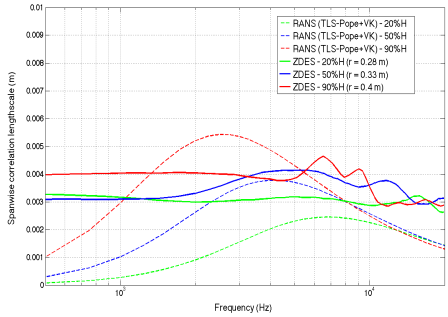

Figure 12. PSD of spanwise correlation length scale obtained from ZDES and compared to RANS-based solutions (using VK model) at 3 height positions.

4. BROADBAND NOISE PREDICTIONS

4.1 Acoustic codes overview

BBN predictions proposed in this work are obtained by chaining the CFD solutions to the two dedicated in-house acoustic codes currently used at ONERA for turbofan noise applications. *TinA*, is based on Amiet isolated airfoil formulation extended to annular cascade configurations by introducing a modal Green's function valid for semi-infinite annular duct and uniform flow, as proposed by Goldstein. 1D and 2D formulations implemented in *TinA* (respectively *TinA1D* and *TinA2D* versions) are detailed in [12]. *TinA* calculations are generally performed using RANS-based inputs [6], but a modified version has been adapted to be chained with ZDES specific outputs. *FanNoise* [12,13], is a frequency domain code currently used to predict tonal and BBN spectra using a FWH analogy (restricted to the loading noise term) and adopting a modal Green's function too. The required inputs are the unsteady pressure harmonics at the blade (rotor sources) or vane (stator sources) walls. BBN predictions related to RSI mechanism are practically obtained by using ZDES turbulent wall pressure extracted over the vane walls.

4.2 Amiet-based predictions using ZDES inputs

BBN predictions based on Amiet theory are first presented in this section. As explained previously, one of the objectives of using scale-resolved turbulence solutions is to evaluate current BBN predictions using isotropic turbulence spectrum models with main turbulence parameters (TI and TLS) deduced from RANS calculations, as done in [6]. Indeed, turbulent wake spectral analyses presented in Section 3.3 have been used to directly feed the Amiet-based code *TinA*. Basically, the acoustic field is linked directly to the 2-wave number turbulence energy spectrum, $\phi_{u_n u_n}$, which can be related to the PSD of upwash velocity, $S_{u_n u_n}$, and to the spanwise correlation length scale (ℓ_r) as [5, 14]:

$$\phi_{u_n u_n}(k_c,k_r) = \frac{U_c}{\pi} S_{u_n u_n}(f)\,\ell_r(f,k_r) \tag{3}$$

$$\ell_r(f,k_r) = \int_0^\infty \gamma(f,r_{12})\cos(k_r r_{12})\,dr_{12} \tag{4}$$

These quantities can be directly obtained from the ZDES, as done here by restricting to the parallel gusts:

$$\phi_{u_n u_n}(k_c,0) = \frac{U_c}{\pi} S_{u_n u_n}(f)\,\ell_r(f) \tag{5}$$

In order to get more reliable predictions, turbulent fields similar as those analysed in Section 3 at HW1 position have been extracted over a plane aligned the OGV leading edge (as done with the RANS inputs too). The corresponding BBN predictions in terms of PWL spectra in the bypass duct are presented in Fig. 13 (red curve). RANS-informed solutions obtained using conventional Pope-based TLS and issued from *TinA1D* (blue dashed line) and *TinA2D* (blue thick line) are plotted too. As known from previous studies, RANS-informed solutions using *TinA1D* tend to overpredict the level in the low and medium frequency range whereas *TinA2D* predictions are expected to be more reliable. A first point to notice is that the peak level frequency is well captured when using the ZDES inputs whereas the one issued from RANS-based *TinA1D* solution is clearly shifted to a lower frequency. Moreover, PWL provided by ZDES-based predictions is surprisingly close to the RANS-based *TinA2D* solution, despite the fact that respective TI and TLS profiles were found to be significantly different. Some balancing effects might certainly explain this result. The ZDES-based solution seems to better fit the experiment in the low frequency range, but this is partly due to non-fully reliable numerical correlation length scales for which uncertainties are growing up at lowest frequencies (see Fig. 12). It would be quite interesting to check the effect of using Eq. (4) instead of Eq. (5) in the ZDES-based BBN predictions, but the numerical assessment of the complete 2-wavenumber turbulence energy spectrum using available ZDES data set is not so easy. Anyway, from these first acoustic results, it seems reasonable to say that isotropic assumptions and von-Karman turbulence spectrum models adopted in the current RANS-informed approaches are not invalidated by the present scale-resolved turbulence investigations.

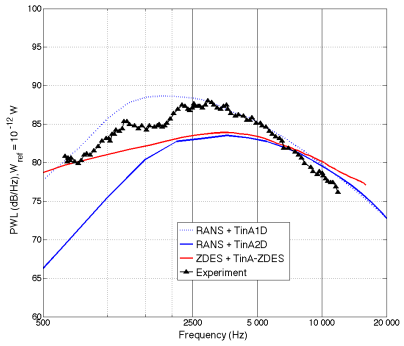

Figure 13. PWL spectra (bypass) provided by *TinA* code using RANS and ZDES inputs extracted at OGV plane and compared to AneCom experiment.

4.3 FWH predictions using ZDES inputs

In this Section, the first BBN predictions obtained using the FWH analogy with direct source inputs are discussed. ZDES data extracted at the vane wall are post-processed to feed the in-house code *FanNoise*, requiring to perform a Fourier transform of the turbulent pressure over the available signal duration. Practically, PSD are calculated from a single Fourier transform of the whole signal without statistical averaging, and a post frequency-band averaging is applied afterwards to reduce the level oscillations. RMS pressure fields over the vane surface are good indicators to check the convergence of the ZDES solution and to visualize the distribution of dominant sources, expected to be mainly located in the

leading edge region. In Fig. 14, RMS wall pressure contour map over the vane suction side issued from ZDES post-processing (Fig. 14, right) is compared to a complementary numerical prediction (Fig. 14, left), obtained using a linearized Euler CAA solver with synthetic turbulence injection [13] (achieved in a dedicated task of TurboNoiseBB project). As expected, dominant sources are found to be concentrated in the leading-edge region with comparable levels (same scales are used). However, it can be noticed that the ZDES solution displays a source field spreading over the entire suction side with significant levels up to the trailing edge, whereas the CAA predicted levels are much more confined to the leading edge region (a similar observation has been made on the pressure side). Moreover, a few high-level spots are visible in the tip region for the ZDES solution. These additional sources are questionable here: they might be due to numerical noise generated at the sliding grid interface (as previously revealed by flow visualizations shown in Fig. 3, right). Another possible issue might be a numerical reflection at the exit boundary, although the ZDES grid cells are properly stretched in this region in order to increase the numerical dissipation (as explained in Section 2). Back-scattered incoming acoustic waves emitted from the exit boundary could pollute the turbulent wall pressure field. These two suspected causes of noise pollution are currently under investigation.

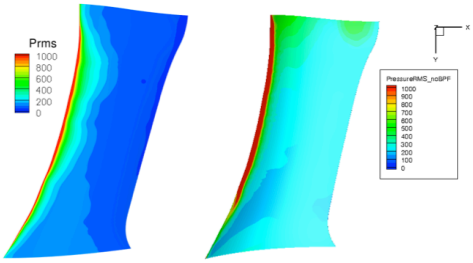

Figure 14. RMS wall pressure maps on vane suction side issued from CAA (left, from [15]) & ZDES (right).

PWL spectra in the bypass duct obtained with ZDES+FWH method are presented in Fig. 15 and compared to the experiment. The predicted levels are clearly over-estimated and reveal the presence undesirable tones with two high-level bumps (centred around 6500 Hz and 9200 Hz).

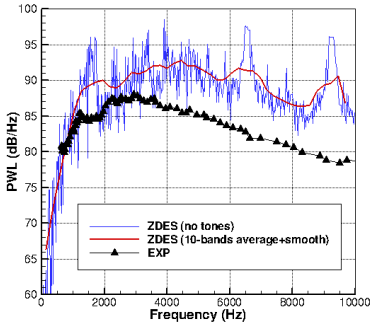

Figure 15. PWL spectra (bypass) issued from ZDES + FWH analogy (*FanNoise*) and compared to experiment

A filtering of these tones combined with a 10-band averaging with a smoothing process is applied on the raw predictions, giving rise to the smoothed spectrum plotted in red line. Despite a drastic reduction of oscillating levels, the predicted levels are about 5-10 dB above the experimental ones, with deviations increasing with frequency. This result is quite disappointing and seems to confirm the presence of additional sources certainly due to numerical artefacts. In order to try to remove the contribution of these non-physical sources, the FWH surface integration is simply restricted to half a chord from the leading edge, as illustrated in Fig. 16, left. This 50% reduction is approximate, but it is a good way to evaluate the contribution of spurious sources (as noise generated by this truncated region should be low). The resulting solution is shown in Fig. 16 right, for raw and averaged/smoothed PWL spectra. A clear benefit can be observed, in particular for mid-frequency and high-frequency levels (beyond 3000 Hz), for which levels are significantly reduced and getting much closer to the expected ones. The frequency range of the spectrum in less impacted by this surface truncation, which is a good point since the initial levels were not so far from the measurements. It tends to show that the numerical noise contribution is quite important in this truncated region of the vane.

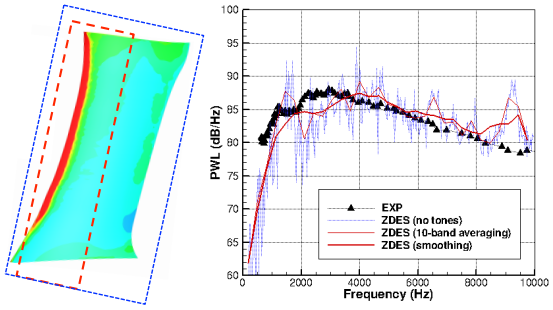

Figure 16. Illustration of restricted FWH integration surface (left) and PWL spectra obtained with mid-chord integration and compared to experiment (right).

Sensitivity to truncation extent has been studied by performing two additional calculations and applying 40% and 30% chord integration, with corresponding results plotted (for the three truncated cases) in Fig. 17, left. Shapes of the spectra are almost similar and levels are getting lower as reducing the integration surface (more particularly for 30% chord integration). Hence, it is actually not possible to ensure a fully reliable prediction and a reasonable compromise at 40% chord is retained in Fig. 17 (right), for comparisons with Amiet predictions using RANS-based and ZDES-based inputs, using a Log axis scale. A good agreement is observed at low frequencies with the RANS+Amiet solution, and all predictions are matching well in the mid-range. Although level oscillations are still present in the ZDES+FWH spectrum at higher frequencies, this solution seems to better capture the attenuation slope from experiment.

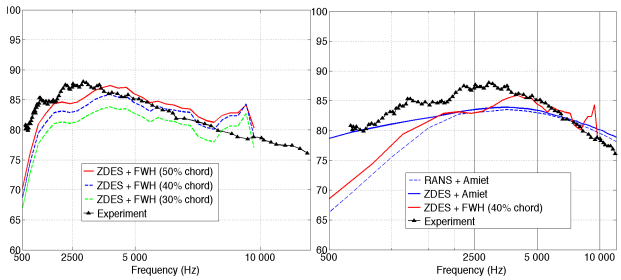

Figure 17. PWL spectra (dB/Hz) obtained from ZDES+FWH calculations using 50%, 40%, 30% chord integration (left), and compared (40% chord int.) to RANS-based solution and experiment (Log scale, right).

5. CONCLUSIONS

A ZDES approach has been conducted to simulate the turbulent flow and BBN power spectra of the ACAT1 fan-OGV stage, at approach conditions. Turbulent wake characteristics have been first analysed and compared to available HW measurements from AneCom test rig (focusing at mid-distance between fan and OGV). Radial profiles of turbulent velocity components are found quite close to the measurements when suited corrections (related to HW probes cut-off frequency around 8 kHz) are applied. The energy of turbulent wakes is shown to be roughly isotropic in the ZDES and in the experiment too. Turbulent velocity spectra show a reasonable agreement with the experiment (up to the HW cut-off frequency) and not far from usual isotropic turbulence von-Karman spectrum models when adjusting TI and TLS values. Estimates and analyses of integral and spanwise correlation length scales have been discussed in order to provide relevant information aiming to feed in-house acoustic tools. Hence, first BBN predictions based on Amiet approach (using RANS-based and ZDES-based turbulent wake characteristics extracted just upstream the OGV) and FWH analogy with loading noise source terms (using turbulent wall pressure over the OGVs surface directly provided by ZDES) have been performed and discussed. Following comments can be pointed out:

- Numerical noise created at the sliding grid interface has been detected and is partly responsible for a pollution of turbulent pressure at the vane wall, also attributed to possible numerical reflections at the exit boundary of the CFD domain.
- Nevertheless, all the studied methods provide satisfactory estimations of PWL spectra in terms of shape and levels with overall deviations within 3 dB from each other and less than 5 dB from experiment.
- Despite a better capture of turbulent wake characteristics, the benefit of using direct ZDES inputs in Amiet-based predictions is not clearly addressed yet.
- ZDES+FWH direct method is certainly the most promising one, and its feasibility has been demonstrated, but the presence of additional spurious sources does not permit a fully reliable assessment of PWL spectra.
- RANS-informed solutions are still competitive and seem rather reliable regarding the present results, at least as long as scale-resolved turbulence methods are not getting more robust and not clearly addressing a much better accuracy in BBN predictions.

ACKNOWLEDGEMENTS

The presented work was conducted in the frame of the project TurboNoiseBB, with funds from the European Union's Horizon 2020 research and innovation program under grant agreement No. 690714. Access to HPC resources was allocated by GENCI (French National Computing Center). The authors would like to thank DLR team for providing the experimental data set.

6. REFERENCES

[1] B. François, R. Barrier, C. Polacsek, "Zonal Detached Eddy Simulation of the Fan-OGV Stage of a Modern Turbofan Engine", submitted and accepted for *ASME TurboExpo2020*, London (UK), June 2020.

[2] S. Guérin, C. Kissner, B. Kajasa, R. Jaron, M. Behn, S. Hakansson, B. Pardowitz, U. Tapken, R., Meyer, and L. Enghardt, "Noise prediction of the ACAT1 fan with a RANS-informed analytical method: success and challenge", *25th AIAA/CEAS Aeroacoustics Conference, AIAA-2019-2500*, 2019.

[3] D. Casalino, A. Hazir, A. Mann, "Turbofan Broadband Noise Prediction Using the Lattice Boltzmann Method", *AIAAJ, vol. 56(2)*, 2018.

[4] C. P. Arroyo, T. Leonard, M. Sanjose, S. Moreau, and F. Duchaine, "Large Eddy Simulation of a Scale-Model Turbofan for Fan Noise Source Diagnostic", *Journal of Sound and Vibration, **445***, pp. 64–76, 2019.

[5] V. Bonneau, C. Polacsek, L. Castillon, J. Marty, Y. Gervais, and S. Moreau, "Turbofan Broadband Noise Predictions using a 3-D ZDES Rotor Blade Approach", *22nd AIAA/CEAS Aeroacoustics Conference*, *AIAA-2016-2950*, 2016.

[6] S. Guérin et al., "ACAT1 Benchmark of RANS-informed Analytical Methods for Fan Broadband Noise Prediction: Part II - Influence of the Acoustic Models", submitted to *26th AIAA/CEAS Aeroacoustics Conference*, 2020.

[7] S. Deck, "Recent Improvements in the Zonal Detached Eddy Simulation (ZDES) Formulation", *Theoretical and Computational Fluid Dynamics, **26***(6), pp. 523–550, 2012.

[8] L. Cambier, S. Heib, S. Plot, "The Onera elsA CFD Software: Input from Research and Feedback from Industry", *Mechanics & Industry, **14***(3), 2013.

[9] S.B. Pope, "Turbulent Flows", *Cambridge Univ. Press,* England, U.K., 2000.

[10] R. Jaron, H. Herthum, M. Franke, A. Moreau, S. Guérin, "Impact of Turbulence Models on RANS-Informed Prediction of Fan Broadband Interaction Noise", *ETC12*, April 2017.

[11] D.A. Lynch, T.J. Mueller, and W.K. Blake, "A Correlation Length Scale for the Prediction of Aeroacoustic Response", *AIAA-2002-2569*, 2002.

[12] G. Reboul, C. Polacsek, S. Lewy, and S. Heib, "Ducted-fan broadband noise simulations using unsteady or averaged data", Inter-noise2008, 2008.

[13] A. Cader, C. Polacsek, T. Le Garrec, R. Barrier, B. François, "Numerical prediction of rotor-stator interaction noise using 3D CAA with synthetic turbulence injection", *24th AIAA/CEAS Aeroacoustics Conference*, Dallas (USA), 2018.

[14] J. Winkler, S. Moreau, T. Carolus, "Airfoil trailing-edge blowing: broadband noise prediction from Large-Eddy Simulation", *AIAA Journal, vol. 50(2), pp. 294–303*, 2012.